

Creating an Antibacterial with in Vivo Efficacy: Synthesis and Characterization of Potent Inhibitors of the Bacterial Cell Division Protein FtsZ with Improved Pharmaceutical Properties

David J. Haydon,^{*,†} James M. Bennett,[†] David Brown,[†] Ian Collins,[†] Greta Galbraith,[†] Paul Lancett,[†] Rebecca Macdonald,[†] Neil R. Stokes,[†] Pramod K. Chauhan,[‡] Jignesh K. Sutariya,[‡] Narendra Nayal,[‡] Anil Srivastava,[‡] Joy Beanland,[§] Robin Hall,[§] Vincent Henstock,[§] Caterina Noula,[§] Chris Rockley,[§] and Lloyd Czaplewski[†]

[†]*Biota Europe Ltd., Begbroke Science Park, Sandy Lane, Yarnton, Oxfordshire OX5 1PF, U.K.*, [‡]*Jubilant Chemsys Ltd., B-34, Sector-58, Noida 201301, India*, and [§]*Key Organics Ltd., Highfield Industrial Estate, Camelford, Cornwall PL32 9QZ, U.K.*

Received November 5, 2009

3-Methoxybenzamide (**1**) is a weak inhibitor of the essential bacterial cell division protein FtsZ. Alkyl derivatives of **1** are potent antistaphylococcal compounds with suboptimal drug-like properties. Exploration of the structure–activity relationships of analogues of these inhibitors led to the identification of potent antistaphylococcal compounds with improved pharmaceutical properties.

Introduction

Multidrug-resistant strains of Gram-positive pathogens have evolved which are especially difficult to eradicate. In particular, the emergence and spread of multidrug-resistant *Staphylococcus aureus* is a serious health concern.^{1,2} Subsequently, there is a continuing need for alternative antibacterial agents, especially with novel mechanisms of action. The increasing use of methicillin resistant *S. aureus* screening with rapid diagnostics³ prior to elective hospital admissions means that a selective antistaphylococcal agent would be a useful addition to the clinician's armory.

Cell division has been of considerable interest to the pharmaceutical industry as a target because it involves a group of well-conserved proteins that are all essential for the viability of a wide range of bacteria, and their activities are distinct from those of the proteins involved in mammalian cell division.^{4,5} FtsZ is an essential guanosine triphosphatase that undergoes GTP-dependent⁶ polymerization at midcell and assembles to form the Z-ring. When bacteria divide, FtsZ recruits other cell division proteins to synthesize the septum that enables the daughter cells to separate. FtsZ is structurally and functionally homologous to mammalian β -tubulin, which has been successfully exploited for cancer therapy.^{6–8} This suggests that FtsZ may also be amenable to inhibitor development.

Several compounds have been reported to block bacterial cell division through inhibition of FtsZ.^{4,9,10} Many of these reported inhibitors were explored, and 3-methoxybenzamide

(compound **1**) was found to be the most attractive for development into an antibacterial agent. Recently, we reported the identification of a potent derivative of **1**, PC190723 (Figure 1, compound **2**), that inhibits FtsZ, resulting in enlargement of the bacterial cells (Figure 2) and killing of staphylococci in vivo.¹¹

The early structure–activity relationships (SAR) leading to the synthesis of potent 2,6-difluoro-3-alkoxybenzamide FtsZ inhibitors from **1** has been published.¹² These 2,6-difluoro-3-alkoxybenzamides are 8000 \times more potent than **1**¹² and are excellent reagents to explore bacterial cell biology. To be clinically efficacious, a compound must have appropriate physicochemical properties¹³ so that it is absorbed, distributed, and not extensively metabolized or rapidly excreted. The 2,6-difluoro-3-alkoxybenzamides have suboptimal drug-like absorption, distribution, metabolism, or excretion (ADME) properties, so the objective was to improve the pharmaceutical profile of these FtsZ inhibitors while retaining the on-target antistaphylococcal activity to create molecules suitable for preclinical development.

The SAR and the process used to create **2**, a compound with attractive in vivo pharmacology, from the 2,6-difluoro-3-alkoxybenzamide FtsZ inhibitors that have antibacterial activity, but suboptimal drug-like properties, are described here.

Chemistry

The routes to the target 3-substituted 2,6-difluoro-benzamide analogues are concise, straightforward, and are described below. The commercially available 2,6-difluoro-3-methoxybenzamide (**3**) was demethylated to the phenol (**4**) via treatment with boron tribromide in dichloromethane. The synthesis of most final compounds was achieved via alkylation of **4** with an alkyl halide in the presence of potassium carbonate with dimethylformamide as solvent (Schemes 1 and 2). In the case of compounds **6j** and **6k**, the alkylation of **4** with the corresponding alcohols was performed under Mitsunobu reaction conditions, using triphenyl phosphine and diisopropyl azodicarboxylate (DIAD) in tetrahydrofuran (THF) (Scheme 2).

*To whom correspondence should be addressed. Phone: +441-865854700. Fax: +441865854799. E-mail: d.haydon@biota.com.au.

^aAbbreviations: ADME, absorption, distribution, metabolism and excretion; APCI, atmospheric pressure chemical ionization; AUC, area under the curve; BSA, bovine serum albumin; CFU, colony forming units; DIAD, diisopropyl azodicarboxylate; DMF, dimethylformamide; DMSO, dimethyl sulfoxide; ESI, electrospray ionization; GTP, guanosine triphosphate; HPLC, high pressure liquid chromatography; IP, intraperitoneal; IV, intravenous; LC, liquid chromatography; MIC, minimal inhibitory concentration; MS, mass spectrometry; NMR, nuclear magnetic resonance; PO, per oral; PK, pharmacokinetics; *R*_t, retention time; SAR, structure–activity relationship; SC, subcutaneous; THF, tetrahydrofuran; TLC, thin layer chromatography; UV, ultraviolet.

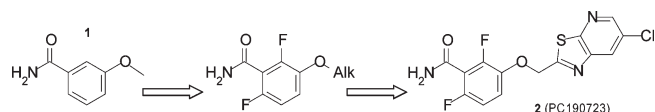


Figure 1. Design of analogues leading toward **2**.

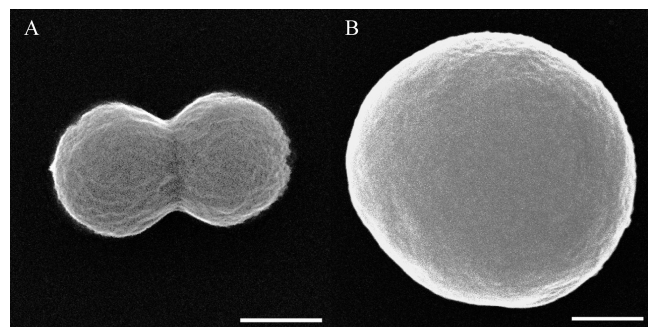
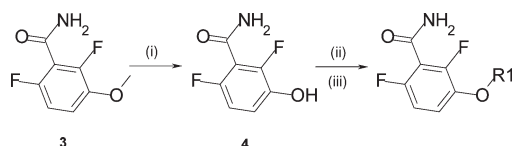


Figure 2. Electron micrographs of *S. aureus* showing cell enlargement following treatment with compound **2**. Cells of *S. aureus* ATCC 29213 were cultured (3 h) in the absence (A) or presence (B) of 2 $\mu\text{g}/\text{mL}$ of compound **2** and analyzed by electron microscopy. *S. aureus* balloons in response to exposure with cell division inhibitors. Scale bars = 0.5 μm .

Scheme 1. General Synthetic Scheme^a



^a Reagents and conditions: (i) demethylation: BBr_3 , CH_2Cl_2 ; (ii) alkylation of phenol using alkyl halides; (iii) alkylation of phenol via Mitsunobu reaction.

A subseries based on the 5-substituted benzothiazol-2-yl methoxy group was accessed by alkylation with a wide range of 5-substituted-2-halomethyl-benzothiazoles (Scheme 3). Further analogues were accessed by standard modification of several 5-position substituents.

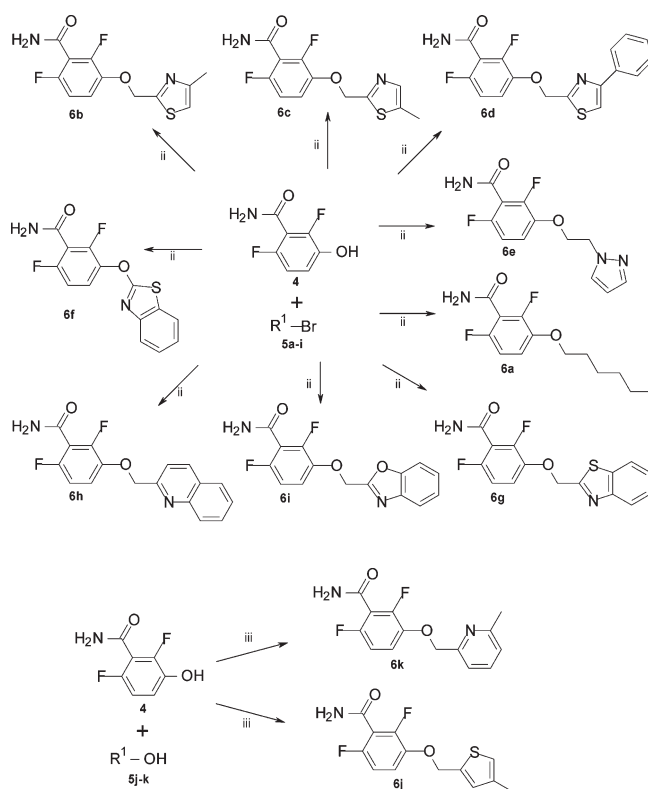
Similarly, a small series of substituted thiazolopyridines was accessed by alkylation with substituted halomethyl-thiazolopyridines and subsequent standard modification (Scheme 6).

For the isomeric 4- and 6-substituted subseries of benzothiazoles, a different approach was used if the suitably substituted 2-halomethyl-benzothiazole was not available. 3-(Cyanomethoxy)-2,6-difluorobenzamide (**19**) was prepared via alkylation of **4** with chloroacetonitrile and served as a common intermediate for the synthesis of compounds **22a–e** (Scheme 4). The 2-amino-1,3-benzothiazoles (**20a–e**) were converted to the required amino thiols (**21a–e**) by refluxing with KOH in aqueous 2-methoxyethanol. These in turn were condensed with **19** in EtOH at 120–150 °C to afford the desired 4-, 6- and 7-substituted benzothiazoles **22a–e**.

Results and Discussion

The biological activities of the compounds were determined by measuring the minimal inhibitory concentrations (MICs) against *S. aureus* ATCC 29213 and by morphometric analysis using light microscopy to determine on-target activity, expressed by ballooning of the cocci.^{11,14} In line with CLSI approved standards, the reproducibility of the MIC test is within one 2-fold dilution of the actual end point.¹⁶ On-target activity was substantiated for selected compounds by generating

Scheme 2. Alkylation of 2,6-Difluoro-3-hydroxybenzamide **4** Using Alkyl Halides (ii; **5a–i**) or via Mitsunobu Reaction (iii; **5j–k**)^a



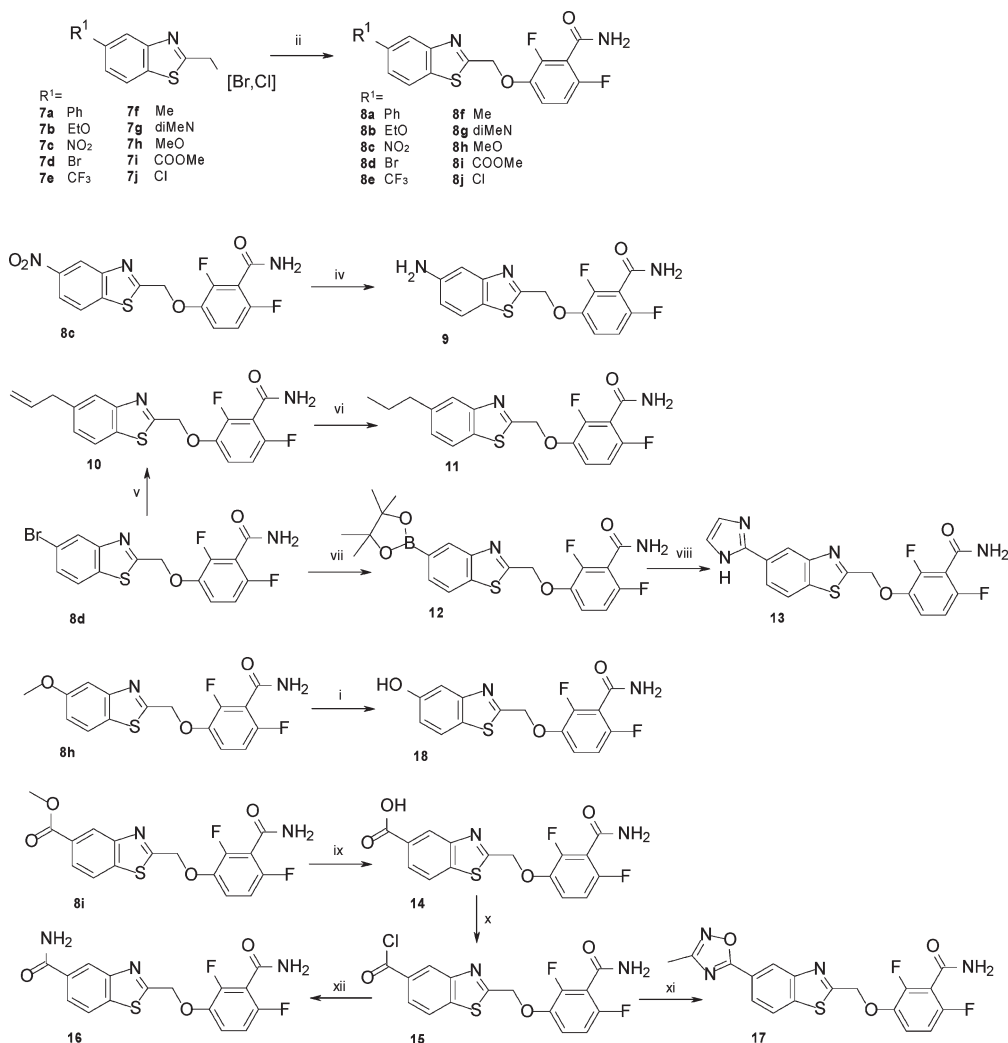
^a Reagents: (ii) K_2CO_3 , DMF; (iii) triphenylphosphine, diisopropyl azodicarboxylate, triethylamine, THF.

compound-resistant strains; in all cases, a mutation was identified in the *ftsZ* gene (data not shown). Selected compounds with a suitable level of on-target activity were screened through a panel of assays to determine their in vitro ADME properties. Compounds with drug-like in vitro ADME profiles were then characterized in vivo.

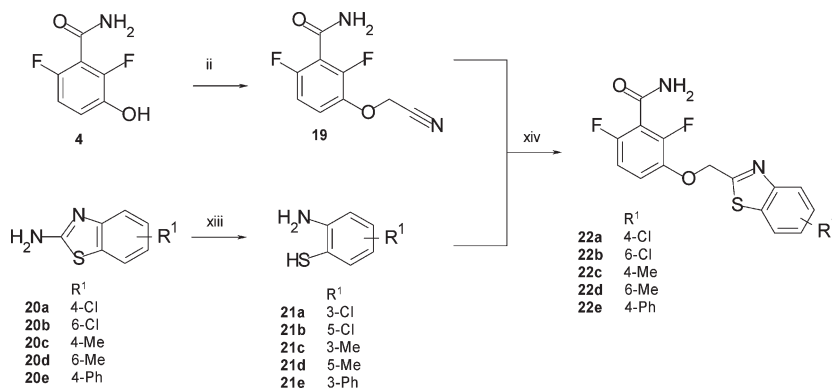
To improve the pharmaceutical properties of the 2,6-difluoro-3-alkoxybenzamide FtsZ inhibitors, a series of molecules where the alkyl substituent was replaced with a heterocycle, were synthesized (Scheme 2). Approximately 60 of this type of molecule were synthesized from commercial building blocks where the molecular weight of R^1 was in the 100–200 Da range. Replacing the alkyl substituent with such heterocycles was designed to reduce the log *P*, the number of rotatable bonds, and the plasma protein binding of the molecule as well as to introduce the potential for additional hydrogen bonding to the FtsZ protein.

The antibacterial activity against *S. aureus* and inhibition of cell division for a selection of this series of 3-substituted 2,6-difluorobenzamides (compounds **6a–k**) is presented in Table 1. Several methoxy-linked heterocyclic derivatives demonstrated potent antistaphylococcal activity mediated through inhibition of cell division. The most potent of these, a benzothiazole compound **6g**, was selected for additional exploration of the SAR. Analogues with substitutions in each of the available positions of the benzothiazole were prepared (Schemes 3, 4, 5).

This series of substituted benzothiazoles were tested for inhibition of cell division and antibacterial activity against *S. aureus* (Table 2). The presence of a chloro substitution in the 4-, 6-, or 7-position of the benzothiazole (compounds **22a**, **22b**, and **24e**) resulted in active compounds but with reduced

Scheme 3. Synthesis of 5-Substituted Benzothiazole Derivatives by Alkylation of 2,6-Difluoro-3-hydroxybenzamide (**4**) Using Alkyl Halides (**7a–7j**)^a


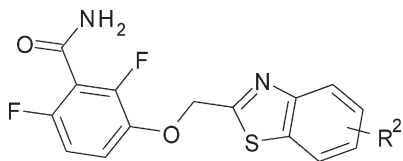
^a Reagents: (i) BBr₃, CH₂Cl₂; (ii) K₂CO₃, DMF; (iv) SnCl₂·2H₂O, EtOH, reflux; (v) allyltributyltin, tetrakis(triphenylphosphine)palladium(0), DMF; (vi) Pd-C, MeOH; (vii) bispinacolatodiboron, KOAc, Pd₂(dba)₃, tricyclohexylphosphine, 1,4-dioxane; (viii) 2-iodoimidazole, dichlorobis(triphenylphosphine)palladium(II), K₃PO₄, DMF-H₂O, 120 °C. (ix) LiOH, THF-H₂O, reflux; (x) SOCl₂, toluene, reflux; (xi) acetamide oxime, K₂CO₃, toluene, reflux; (xii) NH₃ (gas), THF.

Scheme 4. Synthesis of Substituted Benzothiazole Derivatives from 3-Cyanomethoxy-2,6-difluoro-benzamide **19** and Substituted 2-aminobenzenethiols^a


^a Reagents: (ii) chloroacetonitrile, K₂CO₃, DMF; (xiii) ~10 N KOH in 2-methoxyethanol or 10 N NaOH, reflux; (xiv) EtOH at 120–150 °C.

antibacterial activity and potency in the cell division assay. Similarly, 4- and 5-methyl as well as 4-methoxy substitutions of the benzothiazole (compounds **22c**, **8f**, and **25**) resulted

in less potent but active analogues. One compound, with a 5-methoxy substitution (**8h**), retained similar activity to the unsubstituted benzothiazole. From this set of substituted

Table 2. *S. aureus* MICs and Cell Division Inhibitory Activity for a Set of Substituted Benzothiazoles

compd	R ² group	<i>S. aureus</i> MIC (μg/mL)	cell division inhibition ^a (μg/mL)
6g		2	4
22a	4-Cl	16	8
8j	5-Cl	0.25	0.25
22b	6-Cl	4	8
24e	7-Cl	4	8
22c	4-Me	16	2048
8f	5-Me	4	8
22d	6-Me	8	WT
25	4-MeO	16	64
8h	5-MeO	2	2
24b	6-MeO	> 256	WT
22e	4-Ph	> 256	WT
8a	5-Ph	0.25	0.5
24a	6-Ph	> 256	WT
24d	7-Ph	> 256	WT

^aLowest concentration at which ballooning of *S. aureus* is observed indicating on-target activity. WT: No effect on morphology.

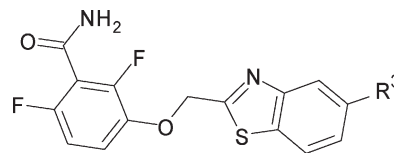
MICs against *S. aureus*. Similarly, methyl ester (**8i**) and 1,2,4-oxadiazol-5-yl (**17**) substitutions resulted in improved on-target activity.

The design of molecules was largely driven by traditional SAR-directed medicinal chemistry processes; however, the availability of FtsZ crystal structures enabled the use of structure-informed optimization of the ligands.

A cleft between helix 7 and the C-terminal domain of FtsZ¹⁵ was identified as a potential binding site for this series of inhibitors (Figure 3).¹¹ The experimental findings described herein are consistent with the proposed binding model with a preference for hydrophobic substitutions and all of the active compounds docked convincingly into the hydrophobic channel present in the *S. aureus* FtsZ protein. The model was not used to design molecules per se, however it was used as a tool to prioritise the synthesis of compounds that docked well into the binding site.

Because of the hydrophobic nature of the molecules, the protein binding was of concern and the effect of protein on the antibacterial activity was tracked by adding protein (50% v/v serum or 2% w/v bovine serum albumin (BSA)) to the MIC assays. The alkyloxy compounds, such as **6a**, were particularly sensitive to the presence of added protein with serum or BSA inducing large fold increases in the MICs. The majority of compounds described herein were less sensitive to added protein, with serum or BSA inducing more modest shifts in the MICs (Tables 1 and 4). Nonetheless, the most active benzothiazole derivatives were still highly bound to protein with plasma protein binding values of > 95% being observed using an equilibrium dialysis assay (Table 4).

Because hydrophobic substituents appear to be preferred from an activity perspective (Table 3), attempts were made to reduce protein binding by lowering the logP without introducing polar groups. As such, a set of thiazolopyridine analogues were synthesized (Scheme 6). The antibacterial activity and

Table 3. *S. aureus* MICs and Cell Division Inhibitory Activity for a Set of 5-Substituted Benzothiazoles

compd	R ³ group	<i>S. aureus</i> MIC (μg/mL)	cell division inhibition ^a (μg/mL)
6g	5-H	2	4
8j	5-Cl	0.25	0.25
8f	5-Me	4	8
11	5-propyl	0.125	0.125
8h	5-MeO	2	2
8b	5-EtO	0.125	0.125
8a	5-Ph	0.25	0.5
8d	5-Br	0.125	0.25
8e	5-CF ₃	0.25	0.5
18	5-OH	32	64
9	5-NH ₂	> 64	WT
8g	5-(dimethylamino)	> 64	WT
16	5-CONH ₂	> 64	WT
14	5-COOH	> 64	WT
8i	5-COOMe	1	2
17	5-(1,2,4-oxadiazol-5-yl)	0.5	0.5
13	5-(imidazol-2-yl)	> 64	WT

^aLowest concentration at which ballooning of *S. aureus* is observed indicating on-target activity. WT: no effect on morphology.

plasma protein binding were determined for these analogues (Table 4).

The thiazolopyridine (**28c**) where Z² = N was 32-fold less active than the benzothiazole (**8j**), however where Z¹ = N (**2**, **30**, and **29**), the antibacterial activity was equivalent or only 2–4-fold less potent than the corresponding benzothiazole. Furthermore, the plasma protein binding of the thiazolopyridines was lower for the chloro (**2**) and ethoxy (**29**) derivatives.

The in vitro ADME properties were determined for molecules where the potency and protein binding were suitable for progression. The upper portion of Table 5 summarizes the results of a set of in vitro screens used to evaluate the drug-like properties of compound **2** with compound **8j** shown for comparison. Standard deviations are shown, where available, to illustrate typical assay variability.

Compound **2** did not inhibit any of the cytochrome P450 isozymes tested, nor did it inhibit the hERG ion channel at the concentrations tested. The chemical and plasma stabilities of compound **2** were good, and the clearances in microsomes and hepatocytes were low, suggesting that it should not be rapidly metabolized in vivo. The permeability of compound **2** in Caco-2 cells was good with a low efflux ratio, indicating that compound **2** should not be a substrate of drug transporters such as P-glycoprotein and should be orally bioavailable. Compound **8j** had a similar ADME profile to compound **2**, with increased plasma protein binding and increased clearance in hepatocytes being the notable exceptions.

Table 5 and Figure 4 illustrate the pharmacokinetic properties of compound **2**, with **8j** shown for comparison. The clearance (CL) of compound **2** following intravenous administration in the mouse was low, with a long terminal half-life (T_{1/2}) resulting in a good area under the curve (AUC). The oral bioavailability of compound **2** was also good at 57%. In

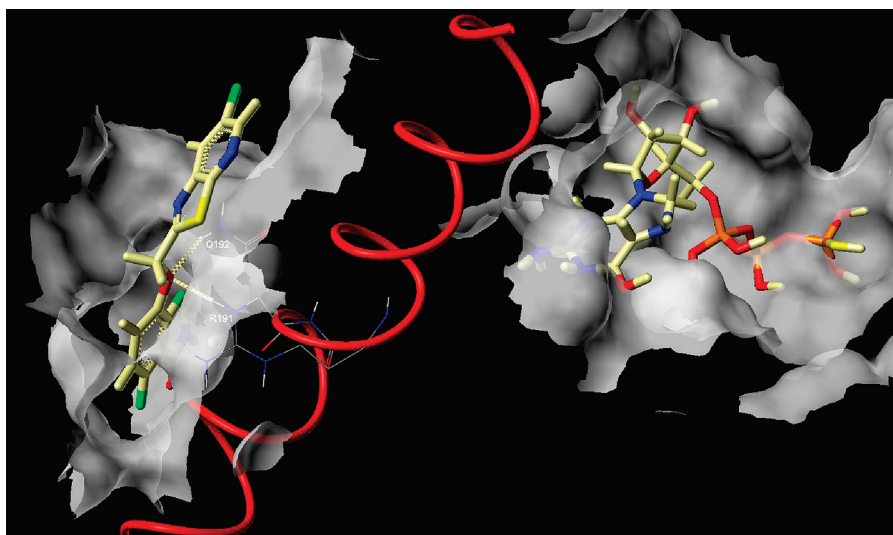
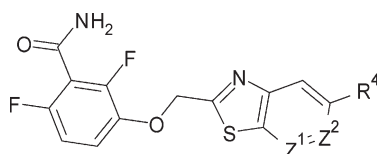


Figure 3. Model of **2** docked into cleft of FtsZ. Close up view showing the nucleotide substrate bound into the nucleotide-binding site (right) and **2** docked into a cleft (left) analogous to the taxol-binding site of tubulin adjacent to helix 7 (red). In this model, hydrogen bonds are formed between the phenoxy ether of **2** and R191 and Q192 (dashed yellow lines).

Table 4. *S. aureus* MICs and Plasma Protein Binding for a Series of Substituted Benzothiazoles and Thiazolopyridines



compd	R ⁴	Z ¹	Z ²	<i>S. aureus</i> MIC (μg/mL)	<i>S. aureus</i> MIC + 2% BSA (μg/mL)	plasma protein binding ^a (% bound)	clogP
8j	Cl	CH	CH	0.25	2	96.4	2.5
2	Cl	N	CH	1	2	85.4	1.4
8a	Ph	CH	CH	0.25	4	99.2	3.4
30	Ph	N	CH	0.5	4	98.5	2.4
8b	EtO	CH	CH	0.125	0.5	96.4	1.9
29	EtO	N	CH	0.125	0.25	89.9	0.9
28c	Cl	CH	N	8	32	nd	1.4
28d	MeO	N	CCl	16	> 64	nd	0.9

^aPercent of compound bound to mouse plasma. nd: not determined.

contrast, the corresponding benzothiazole (compound **8j**) was rapidly cleared both in hepatocytes and in the mouse.

Both compounds **2** and **8j** were tested in a murine model of staphylococcal infection (Figure 5). Compound **2** was efficacious following a single administration: intraperitoneal (IP) ED₅₀ < 3 mg/kg, subcutaneous (SC) ED₅₀ = 7 mg/kg, and intravenous (IV) ED₅₀ = 10 mg/kg.¹¹ While compound **8j** was efficacious when administered IP (ED₅₀ = 41 mg/kg), it was not when administered SC (ED₅₀ > 30 mg/kg). Although the bioavailability of compound **2** was good, no efficacy was observed following a single oral administration of 30 mg/kg (data not shown).

Therefore the modest reduction in potency of the thiazolopyridine compared to the benzothiazole is more than offset by reducing protein binding and metabolism, resulting in a drug-like pharmacokinetic profile and efficacy in the murine model of staphylococcal infection.

Conclusion

A series of 3-substituted benzamides as inhibitors of FtsZ, which demonstrate potent antistaphylococcal activity by

inhibiting cell division, has been synthesized and the SAR has been determined.

Replacement of a 3-alkyloxy substituent with a variety of heteroarylmethoxy substituents resulted in drug-like compounds with on-target antibacterial activity. The most potent of these substitutions was 1,3-benzothiazol-2-ylmethoxy, so the focus was to optimize the benzothiazole by further substitution around the phenyl ring. Substitutions such as chloro, phenyl, or ethyloxy in the 5-position of the benzothiazole resulted in an 8- to 16-fold improvement in the on-target activity, with MICs as low as 0.125 μg/mL against *S. aureus*.

Although these 5-substituted-1,3-benzothiazol-2-ylmethoxy compounds were more drug-like than the 3-alkyloxy derivatives described above, their protein binding, at > 95% bound to plasma, was considered too high to progress. Replacing the benzothiazole substituent with a thiazolopyridine reduced the antibacterial activity but also reduced the plasma protein binding. Furthermore, the metabolic stability of the thiazolopyridine was improved compared to the benzothiazole, resulting

Table 5. ADME Properties and PK Parameters for Compounds **2** and **8j**^a

assay	units	8j	2
CYP1A2 inhibition	IC ₅₀ (μg/mL)	> 12	> 12
CYP2C19 inhibition	IC ₅₀ (μg/mL)	> 12	> 12
CYP2C9 inhibition	IC ₅₀ (μg/mL)	> 12	> 12
CYP2D6 inhibition	IC ₅₀ (μg/mL)	> 12	> 12
CYP3A4 inhibition	IC ₅₀ (μg/mL)	> 12	> 12
chemical stability	% remaining after 24 h	99 ± 5.4	100 ± 10.3
human microsomal stability	CL (μL/min/mg)	nd	7.2 ± 4.4
human plasma stability	% remaining after 24 h	nd	100 ± 5.2
human plasma binding	fraction unbound	0.01 ± 0.01	0.10 ± 0.03
mouse hepatocyte stability	CL (μL/min/10 ⁶ cells)	31.2 ± 2.7	9.51 ± 1.6
mouse microsomal stability	CL (μL/min/mg)	14.0 ± 4.8	14.5 ± 10.3
mouse plasma stability	% remaining after 24 h	99 ± 11.2	94 ± 10.8
mouse plasma binding	fraction unbound	0.03 ± 0.02	0.15 ± 0.06
hERG inhibition	IC ₅₀ (μM)	nd	> 10
Caco-2 permeability	efflux ratio	nd	0.645
Caco-2 permeability	P _{app} AB (cm/s)	nd	48.7
Caco-2 permeability	P _{app} BA (cm/s)	nd	31.4
mouse intravenous PK parameters	dose (mg/kg)	2	3 [3]
[mouse oral PK parameters]	AUC (μg·h/mL)	0.1	2.42 [1.39]
	C ₀ [C _{max}] (μg/mL)	0.5	3.7 [0.7]
	CL (mL/min/kg)	315	20.6
	T _{1/2} [T _{max}] (min)	13	37 [24]
	V (L/kg)	5.8	1.06

^a nd: not determined. ± standard deviations.

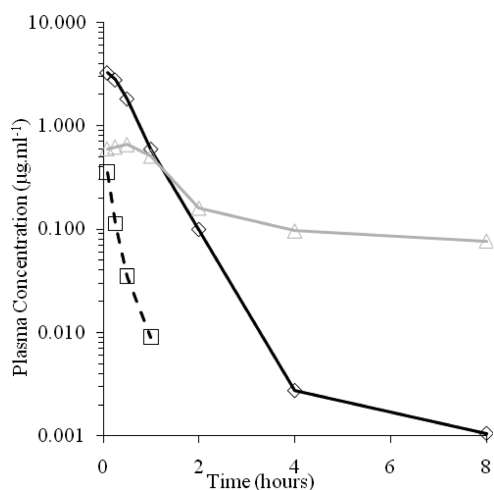


Figure 4. Pharmacokinetic profile of compounds **2** (solid lines) and **8j** (dotted line). Compound **2** was dosed intravenously (black line) and orally (gray line) at 3 mg/kg individually and compound **8j** at 2 mg/kg in a cassette. Plasma concentrations were measured over an 8 h period with samples taken after 5, 15, 30, 60, 120, 240, and 480 min.

in an approximately 15-fold reduction in clearance following intravenous administration in the mouse.

The balance of antibacterial activity, plasma protein binding, and metabolic stability of compound **2** resulted in the compound being tested in the mouse model of staphylococcal infection. Compound **2** was efficacious in an in vivo model of infection, protecting mice infected with a lethal dose of *S. aureus*. The data validate FtsZ as a target for antibacterial intervention and demonstrate that the series is suitable for optimization into a new antistaphylococcal therapy.

Experimental Section

Antimicrobial Testing. *S. aureus* ATCC 29213 was obtained from LGC Promochem (Teddington, UK) and was propagated

according to standard microbiological practice. MICs were determined by the broth microdilution method according to the recommendations of the Clinical and Laboratory Standards Institute.¹⁶ Cell division phenotype assays were performed as described previously.¹⁷

ADME Testing. The cytochrome P450 assay measured the metabolism of fluorogenic substrates by human recombinant enzymes supplied by Invitrogen. The hERG assay, performed at Cypotex Ltd. (Macclesfield, UK), was a single cell planar patch clamp assay. Plasma protein binding was assessed by equilibrium dialysis of a 10 μM solution using the Pierce RED devices. Plasma stability of a 10 μM solution was determined by LC/MS after 24 h at 37 °C. Microsomal stability of a 10 μM solution was determined over a time course by measuring the remaining parent compound using LC/MS. Permeability assays, performed at Cypotex Ltd., used LC/MS/MS to determine bidirectional transport across Caco-2 monolayers. Chemical stability of a 10 μM solution in phosphate buffered saline was determined by LC/MS after 24 h at 37 °C. Hepatocyte stability of a 10 μM solution, performed at Cypotex Ltd., was determined over a time course by measuring the remaining parent compound using LC/MS/MS.

Pharmacokinetics. Parameters were calculated using Win-Nonlin from the plasma concentrations determined by LC/MS/MS over an 8 h time course following intravenous or oral administration of the compounds in mice.

Efficacy. Mice were inoculated IP with an LD_{90–100} of *S. aureus* (Smith) (5 × 10⁵ CFU/mouse for SC study and 4 × 10⁵ CFU/mouse for IP study) in 0.5 mL of brain heart infusion broth containing 5% mucin. Vehicle and test substances were administered SC or IP 1 h after bacterial inoculation. Mortality was monitored for 7 days. The minimal effective dose (ED₅₀) was determined by nonlinear regression using Graph Pad Prism.

Ligand Docking. Docking of ligands to the putative binding site on *Bacillus subtilis* FtsZ described previously¹¹ was completed using Benchware 3D Explorer software (Tripos L.P.).

clogP Calculations. clogP was calculated using Accord for Excel (Accelrys Software Inc.).

Experimental Procedures. All nonaqueous reactions were carried out under nitrogen atmosphere. Reagents and solvents

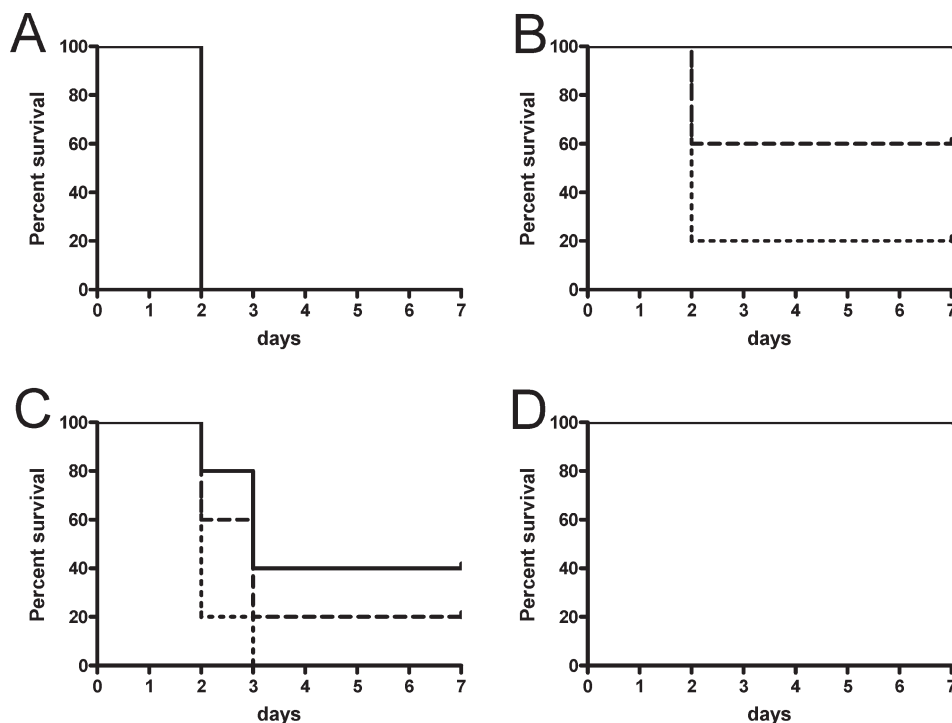


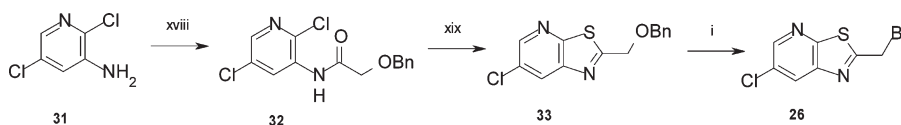
Figure 5. Efficacy of compounds **2** and **8j** in the murine septicaemia model of staphylococcal infection. (A,C) Compound **8j**, (B,D) compound **2**. (A,B) Subcutaneous (SC) administration, (C,D) intraperitoneal (IP) administration. Solid lines = 30 mg/kg, dashed lines = 10 mg/kg, dotted lines = 3 mg/kg. All mice treated with vehicle alone died on day 2. All mice treated SC with 3, 10, or 30 mg/kg of compound **8j** died on day 2 (A). All mice treated IP with 3, 10, or 30 mg/kg of compound **2** survived (D).

were obtained from commercial sources and were used without further purification. 2,6-Difluoro-3-methoxybenzamide (**3**) was purchased from JRD Fluorochemicals Ltd. Yields refer to purified products and are not optimized. Analytical TLC was performed on Merck silica gel 60 F₂₅₄ aluminum-backed plates. Compounds were visualized by UV light and/or stained with either I₂ or potassium permanganate solution followed by heating. Flash column chromatography was performed on silica gel. ¹H NMR spectra were recorded on either a JEOL GSX-400 MHz or on a Bruker Avance 400 MHz spectrometer with a Broad Band Observe (BBO) and Broad Band Fluorine Observe (BBFO) probe. Chemical shifts (δ) are expressed in parts per million (ppm) downfield by reference to tetramethylsilane as the internal standard. Splitting patterns are designated as s (singlet), d (doublet), t (triplet), q (quartet), m (multiplet), br s (broad singlet), app (apparent). Coupling constants (*J*) are given in hertz (Hz). LC-MS analyses were performed on either an Acquity C-18 column (2.10 mm \times 100 mm, 1.70 μ m) using the electrospray ionization (ESI) technique or on a Gemini C-18 column (4.6 mm \times 50 mm, 5 μ m) using the atmospheric pressure chemical ionization (APCI) technique. The purity of all tested compounds was determined by analytical HPLC and HPLC-MS analyses and was greater than 95%, unless otherwise stated. Purity assessment for final compounds was based on the following 5 HPLC methods. Method 1 consisted of the following: Discovery HSC-18 column 4.60 mm \times 250 mm, 5 μ m. Mobile phase; A, acetonitrile with 0.10% formic acid; B, H₂O with 0.10% formic acid; gradient, 10% A to 90% A in 15 min with 30 min run time and a flow rate of 1 mL/min. Method 2 consisted of the following: Purospher Star C-18 column 4.60 mm \times 250 mm, 5 μ m. Mobile phase; A, acetonitrile with 0.10% formic acid; B, H₂O with 0.10% formic acid; gradient, 10% A to 90% A in 15 min with 30 min run time and a flow rate of 1 mL/min. Method 3 consisted of the following: Xbridge C-18 column 4.60 mm \times 250 mm, 5 μ m. Mobile phase; A, acetonitrile with 0.10% formic acid; B, H₂O with 0.10% formic acid; gradient, 10% A to 90% A in 15 min with 30 min run time and a flow rate of 1 mL/min. Method 4

consisted of the following: Acquity BEH C-18 column 2.10 mm \times 100 mm, 1.70 μ m. Mobile phase; A, acetonitrile with 0.10% formic acid; B, H₂O with 0.10% formic acid; gradient, 10% A to 90% A in 6 min with 10 min run time and a flow rate of 1 mL/min. Method 5 consisted of the following: Gemini C-18 column 4.6 mm \times 50 mm, 5 μ m. Mobile phase: 20–90% CH₃CN:10 mM aqueous ammonium acetate, over 4 min, isocratic for 1 min, 20% CH₃CN:10 mM aqueous ammonium acetate for 2 min, flow rate = 1 mL/min at 40 $^{\circ}$ C. Melting points were measured using a Stuart Scientific SMP10 or a Buchi B545 apparatus and are uncorrected. Experimental and spectroscopic details of compounds not described herein and synthetic schemes and experimental details of the intermediates used to make all compounds are presented in the Supporting Information.

2,6-Difluoro-3-hydroxybenzamide (4). Boron tribromide solution (1 M in CH₂Cl₂, 8.55 mL, 8.55 mmol, 2 equiv) was added dropwise to a stirred suspension of 2,6-difluoro-3-methoxybenzamide (**3**) (800 mg, 4.3 mmol) in CH₂Cl₂ (20 mL), at room temperature, under N₂ atmosphere. The reaction mixture was stirred at room temperature for 48 h. The solvent was removed under reduced pressure, and the residue was taken up in water (50 mL) and extracted with EtOAc (3 \times 40 mL). The combined organic extracts were washed with water (2 \times 40 mL), dried (Na₂SO₄), and filtered through a pad of silica. The filtrate was evaporated to dryness under reduced pressure, to give **4** as a light-brown solid (580 mg, 78%). ¹H NMR (DMSO-*d*₆): δ 6.90–6.95 (m, 2H), 7.73 (br s, 1H), 8.03 (br s, 1H), 9.89 (br s, 1H).

2-(Benzyloxy)-N-(2,5-dichloropyridin-3-yl)acetamide (32). To an ice-cold solution of 2,5-dichloropyridin-3-amine (**31**) (2.50 g, 15.33 mmol) in CH₂Cl₂ (50 mL) was added triethylamine (3.17 mL, 23 mmol, 1.5 equiv) followed by the addition of a solution of 2-(benzyloxy)acetyl chloride (4.20 g, 23 mmol, 1.5 equiv) in CH₂Cl₂ (50 mL). The resulting mixture was stirred at room temperature for 2 h. The solvent was removed under reduced pressure, and the residue was taken up in water (100 mL) and extracted with EtOAc (3 \times 100 mL). The combined organic extracts were washed with brine, dried (Na₂SO₄), filtered, and

Scheme 7. Synthesis of the Alkyl Halide Intermediate 26^a

^a Reagents and conditions: (i) BBr₃, CH₂Cl₂; (xviii) 2-(benzyloxy)acetyl chloride, Et₃N, CH₂Cl₂; (xix) Lawesson's reagent, toluene, reflux.

concentrated under reduced pressure. The residue was purified over silica eluting with 5% EtOAc–hexane to obtain the title compound **32** (2.20 g, 46%). LCMS (ESI) 311.04 [M + H]⁺, 84%.

2-[(Benzyloxy)methyl]-6-chloropyrido[3,2-d][1,3]thiazole (33). To a solution of **32** (2.20 g, 7.07 mmol) in toluene (50 mL) was added Lawesson's reagent (2.84 g, 7.07 mmol, 1 equiv), and the resulting reaction mixture was refluxed for 4–5 h. The solvent was evaporated and the residue was purified over silica eluting with 3% EtOAc–hexane to obtain the title compound **33** (1.75 g, 85%). LCMS (ESI) 291.18 [M + H]⁺, 87.50%.

2-(Bromomethyl)-6-chloropyrido[3,2-d][1,3]thiazole (26, Scheme 7). A solution of **33** (2 g, 6.87 mmol) in CH₂Cl₂ (100 mL) was cooled to –78 °C followed by dropwise addition of BBr₃ (3.30 mL, 34.39 mmol, 5 equiv). The mixture was stirred at room temperature for 3 h then was cooled again to –78 °C and quenched by dropwise addition of water followed by extraction with EtOAc (3 × 100 mL). The combined organic extracts were washed with saturated NaHCO₃ solution, dried (Na₂SO₄), filtered, and concentrated under reduced pressure. The residue was purified over silica eluting with 2% EtOAc–hexane to obtain the title compound **26** (1.50 g, 88%). ¹H NMR (DMSO-*d*₆): δ 5.16 (s, 2H), 8.67 (d, *J* = 2.4 Hz, 1H), 8.73 (d, *J* = 2.4 Hz, 1H). MS (ESI) *m/z*: 262.90 [M + H]⁺.

General Procedure for the Alkylation of 4 Using Alkyl or Arylmethyl Halides. K₂CO₃ (1.5–3.5 equiv) and NaI (0.2 equiv) were added to a solution of **4** in DMF (3–8 mL per mmol). The resulting suspension was stirred for 5 min at room temperature before the corresponding halide (1.0–1.1 equiv) was added. The reaction mixture was stirred at 20–60 °C for 3–18 h, under N₂ atmosphere. After cooling to room temperature, one of two workup procedures was followed. In some cases, the reaction mixture was poured into water (15 mL per mmol), and the precipitant solid was filtered, washed with water, and dried to give the crude product. In other cases, the reaction mixture was partitioned between EtOAc (30 mL per mmol) and water (20 mL per mmol), the organic phase was separated, washed with water (2 × 15 mL), dried (MgSO₄), filtered, and concentrated in vacuo to give the crude solid.

3-({6-Chloropyrido[3,2-d][1,3]thiazol-2-yl)methoxy}-2,6-difluorobenzamide (2). Compound **2** was prepared from **4** (590 mg, 3.41 mmol) and **26** (900 mg, 3.41 mmol, 1 equiv) using 3.5 equiv of K₂CO₃, according to the general procedure (20 °C, 3 h, EtOAc/H₂O workup). The residue was purified over silica eluting with 60% EtOAc–hexane to obtain the title compound **2** (940 mg, 78%), mp 218 °C. ¹H NMR (DMSO-*d*₆): δ 5.72 (s, 2H), 7.12 (m, 1H), 7.40 (m, 1H), 7.89 (br s, 1H), 8.17 (br s, 1H), 8.68 (d, *J* = 2.4 Hz, 1H), 8.73 (d, *J* = 2.4 Hz, 1H). MS (ESI) *m/z* 356.27 [M + H]⁺. HPLC (method 3) *R*_t = 15.40 min.

3-(Cyanomethoxy)-2,6-difluorobenzamide (19). Compound **19** was prepared from **4** (1 g, 5.8 mmol) and chloroacetonitrile (0.40 mL, 6.4 mmol, 1.1 equiv) using 1.5 equiv K₂CO₃, according to the general procedure (60 °C, overnight, EtOAc/H₂O workup). The crude product was triturated with diethyl ether (30 mL), filtered, and dried in vacuo to give **19** as a gray solid (1.06 g, 86%); mp 122–123 °C. ¹H NMR (DMSO-*d*₆): δ 5.26 (s, 2H), 7.18 (app dt, *J* = 9.0, 1.8 Hz, 1H), 7.40 (m, 1H), 7.86 (br s, 1H), 8.14 (br s, 1H). HPLC-MS (APCI) *m/z* 213 [M + H]⁺, (method 5) *R*_t = 1.97 min.

General procedure for the synthesis of substituted benzothiazole derivatives from 3-cyanomethoxy-2,6-difluorobenzamide (19) and substituted 1,3-benzothiazol-2-amines. A solution of KOH

(20 equiv) in water (25 mL) was added to a solution of the substituted 1,3-benzothiazol-2-amine in 2-methoxy-ethanol (25 mL), and the reaction mixture was heated to reflux overnight. After cooling at room temperature, the mixture was diluted with water (200 mL), acidified with 5N HCl solution to pH 4, and extracted with CH₂Cl₂ (3 × 150 mL). The combined organic extracts were washed with brine (100 mL), dried (Na₂SO₄), and concentrated under reduced pressure to dryness, to give crude substituted 2-aminobenzethiol. A portion of this material (1.5 equiv) were mixed with **19** (150 mg, 0.7 mmol), and the mixture was stirred at 120 °C, in a preheated oil bath, under N₂, for 2 h. EtOH (2 mL) was added and the reaction mixture was heated at 120 °C for a further 2 h. The products either precipitated from the reaction mixture on cooling or the reaction mixtures were evaporated and the crude products purified by titration of the residue. See the Supporting Information for exact details of each example.

Acknowledgment. We thank S. Ruston for support and D. Davies and various colleagues for assistance and advice. This work was funded by investments from L. Clay and East Hill Management (Boston, MA) and The Wellcome Trust under the Seeding Drug Discovery Initiative.

Supporting Information Available: Synthetic schemes and experimental details of the intermediates used to make the compounds described herein. This material is available free of charge via the Internet at <http://pubs.acs.org>.

References

- (1) Boucher, H. W.; Talbot, G. H.; Bradley, J. S.; Edwards, J. E.; Gilbert, D.; Rice, L. B.; Scheld, M.; Spellberg, B.; Bartlett, J. Bad bugs, no drugs: no ESCAPE! An update from the Infectious Diseases Society of America. *Clin. Infect. Dis.* **2009**, *48*, 1–12.
- (2) Deurenberg, R. H.; Stobberingh, E. E. The molecular evolution of hospital- and community-associated methicillin-resistant *Staphylococcus aureus*. *Curr. Mol. Med.* **2009**, *9*, 100–115.
- (3) Carroll, K. C. Rapid diagnostics for methicillin-resistant *Staphylococcus aureus*: current status. *Mol. Diagn. Ther.* **2008**, *12*, 15–24.
- (4) Vollmer, W. The prokaryotic cytoskeleton: a putative target for inhibitors and antibiotics? *Appl. Microbiol. Biotechnol.* **2006**, *73*, 37–47.
- (5) Lock, R. L.; Harry, E. J. Cell-division inhibitors: new insights for future antibiotics. *Nat. Rev. Drug Discovery* **2008**, *7*, 324–338.
- (6) Löwe, J.; Amos, L. A. Crystal structure of the bacterial cell-division protein FtsZ. *Nature* **1998**, *391*, 203–206.
- (7) Nogales, E.; Wolf, S. G.; Downing, K. H. Structure of the alpha beta tubulin dimer by electron crystallography. *Nature* **1998**, *391*, 199–203.
- (8) Downing, K. H. Structural basis for the interaction of tubulin with proteins and drugs that affect microtubule dynamics. *Annu. Rev. Cell Dev. Biol.* **2000**, *16*, 89–111.
- (9) Ito, H.; Ura, A.; Oyamada, Y.; Tanitame, A.; Yoshida, H.; Yamada, S.; Wachi, M.; Yamagishi, J. H. A 4-aminofurazan derivative-A189-inhibits assembly of bacterial cell division protein FtsZ in vitro and in vivo. *Microbiol. Immunol.* **2006**, *50*, 759–764.
- (10) Paradis-Bleau, C.; Beaumont, M.; Sanschagrin, F.; Voyer, N.; Levesque, R. C. Parallel solid synthesis of inhibitors of the essential cell division FtsZ enzyme as a new potential class of antibacterials. *Bioorg. Med. Chem.* **2007**, *15*, 1330–1340.
- (11) Haydon, D. J.; Stokes, N. R.; Ure, R.; Galbraith, G.; Bennett, J. M.; Brown, D. R.; Baker, P. J.; Barynin, V. V.; Rice, D. W.; Sedelnikova, S. E.; Heal, J. R.; Sheridan, J. M.; Aiwale, S. T.; Chauhan, P. K.; Srivastava, A.; Taneja, A.; Collins, I.; Errington, J.; Czaplowski, L. G. An inhibitor of FtsZ with potent and selective anti-staphylococcal activity. *Science* **2008**, *321*, 1673–1675.

- (12) Czaplowski, L. G.; Collins, I.; Boyd, E. A.; Brown, D.; East, S. P.; Gardiner, M.; Fletcher, R.; Haydon, D. J.; Henstock, V.; Ingram, P.; Jones, C.; Noola, C.; Kennison, L.; Rockley, C.; Rose, V.; Thomaidis-Brears, H. B.; Ure, R.; Whittaker, M.; Stokes, N. R. Antibacterial alkoxybenzamide inhibitors of the essential bacterial cell division protein FtsZ. *Bioorg. Med. Chem. Lett.* **2009**, *19*, 524–527.
- (13) Leeson, P. D.; Springthorpe, B. The influence of drug-like concepts on decision-making in medicinal chemistry. *Nat. Rev. Drug Discovery* **2007**, *6*, 881–890.
- (14) Pinho, M. G.; Errington, J. Dispersed mode of *Staphylococcus aureus* cell wall synthesis in the absence of the division machinery. *Mol. Microbiol.* **2003**, *50*, 871–881.
- (15) Oliva, M. A.; Trambaiolo, D.; Löwe, J. Structural insights into the conformational variability of FtsZ. *J. Mol. Biol.* **2007**, *373*, 1229–1242.
- (16) Clinical and Laboratory Standards Institute. *Methods for Dilution Antimicrobial Susceptibility Tests for Bacteria That Grow Aerobically*; Approved Standard, 7th ed.; CLSI document M07-A7; Clinical and Laboratory Standards Institute: Wayne, PA, 2006.
- (17) Stokes, N. R.; Sievers, J.; Barker, S.; Bennett, J. M.; Brown, D. R.; Collins, I.; Errington, V. M.; Foulger, D.; Hall, M.; Halsey, R.; Johnson, H.; Rose, V.; Thomaidis, H. B.; Haydon, D. J.; Czaplowski, L. G.; Errington, J. Novel inhibitors of bacterial cytokinesis identified by a cell-based antibiotic screening assay. *J. Biol. Chem.* **2005**, *280*, 39709–39715.